

Tumor-associated Antigen L6 and the Invasion of Human Lung Cancer Cells¹

Yu-Rong Kao, Jin-Yuan Shih, Wei-Chun Wen, Ya-Ping Ko, Bing-Mae Chen, Yi-Lin Chan, Yi-Wen Chu, Pan-Chyr Yang, Cheng-Wen Wu, and Steve R. Roffler²

Institute of Biomedical Sciences, Academia Sinica, Taipei, Taiwan 115 [W.-C. W., Y.-P. K., B.-M. C., Y.-L. C., P.-C. Y., S. R. R.]; National Health Research Institutes, Taipei, Taiwan 115 [Y.-R. K., Y.-W. C., P.-C. Y., C.-W. W.]; and Department of Internal Medicine, National Taiwan University Hospital, Taipei, Taiwan 100 [J.-Y. S., P.-C. Y.], Republic of China

ABSTRACT

Metastasis is a coordinated process that depends on the interaction of cancer cells with the tumor microenvironment. Members of the transmembrane-4 superfamily (TM4SF) of surface proteins have been implicated in the regulation of cancer cell metastasis, and the expression of several TM4SF members on tumor cells is inversely correlated with patient prognosis. The tumor-associated antigen L6 (TAL6), a distant member of the TM4SF, is expressed on most epithelial cell carcinomas and is a target for antibody-mediated therapy. We examined whether TAL6 may play a role in cancer metastasis by using an established series of human lung carcinoma cell lines (CL1-0 to CL1-5) that exhibit increasing invasiveness *in vitro* and *in vivo*. We found that TAL6 expression correlated with the *in vitro* invasiveness of CL lung carcinoma cells ($r^2 = 0.98$) and human carcinoma cells ($r^2 = 0.69$). Forced expression of TAL6 on CL1-0 lung carcinoma cells significantly increased their *in vitro* invasiveness and decreased the survival of SCID mice in an experimental metastasis model. Specific antibody against TAL6 (monoclonal antibody L6) significantly reduced the migration and invasiveness of CL1-5 lung carcinoma cells. The effects of monoclonal antibody L6 on CL1-5 invasion required clustering of TAL6 on the cell surface. Real-time reverse transcription-PCR of lung cancer specimens showed that increased expression of TAL6 was significantly associated with early postoperative relapse ($P = 0.034$) and shorter survival ($P = 0.025$) in squamous cell

lung cancer patients. Thus, TAL6 appears to be involved in cancer invasion and metastasis.

INTRODUCTION

Cancer metastasis is a complicated process involving a coordinated program of events that include changes in cell adhesion, polarized proteolysis and migration, intravasation into the circulation, subsequent adhesion to endothelial cells followed by extravasation, invasion, and induction of angiogenesis (1). Cell surface proteins and receptors are intimately involved in these processes. For example, loss of E-cadherin can reduce cell-cell adhesion and allow cancer cells to more readily escape tumors (2). Integrins play vital roles in regulating cell adhesion, motility, invasion, and angiogenesis (3–5), and metalloproteinases on tumor cells can degrade the ECM (6). Other surface proteins including receptor tyrosine kinases (7) and chemokine receptors (8) have been implicated in cancer metastasis. Although much has been learned about how surface proteins influence metastasis, the contribution of many receptors to the metastatic process remains poorly defined.

Tumor-associated antigen L6 is a distant member of the tetraspanin family (9) that was originally identified by mAb³ L6 (10). Members of the tetraspanin or TM4SF (5) of cell surface proteins possess four highly conserved hydrophobic transmembrane domains that form a small and large extracellular loop, a short cytoplasmic loop, and short NH₂ and COOH termini (11). TM4SF members such as CD9, CD63, CD82, and CD151 have been shown to regulate cancer cell motility and metastasis (12–15). The expression of tetraspanins has also been correlated with patient prognosis and survival (16–18).

TAL6 is expressed on most human lung, colon, breast, and ovarian tumors (10), and has generated interest as a target for antibody-mediated therapy (19–21). However, the biological function of TAL6 is largely unknown. TAL6 was found to be highly expressed on an invasive spermatogonia-derived cell line as compared with a noninvasive spermatocyte-derived cell line (22). We picked up TAL6 in a cDNA microarray screen for metastasis-associated genes (23), and TAL6 was reported recently to be involved in the migration of human keratinocytes (24). These findings and the strong association of several TM4SF proteins with cell motility suggested that TAL6 might also be involved in tumor cell metastasis. We used a human lung carcinoma model described previously that includes cell lines displaying different invasive and metastatic capabilities (CL1-0

Received 9/9/02; revised 2/20/03; accepted 3/11/03.

The costs of publication of this article were defrayed in part by the payment of page charges. This article must therefore be hereby marked *advertisement* in accordance with 18 U.S.C. Section 1734 solely to indicate this fact.

¹Supported by a grant (NHRI89A1-PPLABADO1) from the National Health Research Institutes, Taipei, Taiwan.

²To whom requests for reprints should be addressed, at Institute of Biomedical Sciences, Academia Sinica, Yen Ge Yuan Road, Section 2, No. 128, Taipei, Taiwan 115, Republic of China. Phone: 886-2-2652-3079; Fax: 886-2-2782-9142; E-mail: sroff@ibms.sinica.edu.tw.

³The abbreviations used are: mAb, monoclonal antibody; ECM, extracellular matrix; GAM, goat antimouse antibody; GAR, goat antirabbit antibody; MF, mean fluorescence; mAb L6, anti-TAL6 monoclonal antibody L6-20-4; RF, relative fluorescence; SCID, severe combined-immune deficiency; TM4SF, transmembrane-4 superfamily; RT-PCR, reverse transcription-PCR; TBP, TATA-box binding protein; C_T, threshold cycle.

and the sublines CL1-1 to CL1-5; Ref. 25) to study possible roles of TAL6 in lung cancer metastasis. We present data supporting the idea that TAL6 plays a role in cancer cell migration and invasion.

MATERIALS AND METHODS

Cell Lines. Human lung carcinoma cell lines with different invasive and metastatic capabilities (CL1-0 and its sublines CL1-1 to CL1-5) have been described (25). HT-1197 human bladder carcinoma (CRL-1473), Colo320 human colon carcinoma (CL-188), and NCI-H520 human lung carcinoma (HTB-182) cells were obtained from the American Type Culture Collection (Manassas, VA). H928 lung carcinoma cells were a gift from Dr. Ming-Yang Yeh, Cheng Hsin General Hospital, Taipei, Taiwan. NTU-B1 bladder carcinoma cells and SV40-immortalized normal human bronchial epithelial cells (BEAS-2B S-10; Ref. 26) were from Dr. Pan-Chyr Yang, Department of Internal Medicine, National Taiwan Medical School, Taipei, Taiwan. OVTW-59 ovary carcinoma cells were generously provided by Dr. Chin-Tarn Lin, Department of Pathology, National Taiwan Medical School, and EJ bladder carcinoma cells were a gift from Dr. M'liss A. Hudson, Washington University School of Medicine, St. Louis, MO. All of the cells were cultured at 37°C, 5% CO₂ in RPMI 1640 supplemented with 10% bovine serum, 2.98 g/liter HEPES, 2 g/liter NaHCO₃, 100 units/ml penicillin, and 100 µg/ml streptomycin. All of the cells were free of *Mycoplasma* as determined by a PCR-based *Mycoplasma* detection kit (American Type Culture Collection). The effect of antibodies (20 µg/ml) on the growth of CL1-5 cells was determined by counting the cells in triplicate wells every 24 h. Doubling times were calculated by linear regression analysis.

Antibodies. Hybridomas producing anti-TAL6 (L6-20-4), anti-influenza virus A nucleoprotein (HB65), and antihepatitis B virus surface antigen (H25B10) antibodies were obtained from the American Type Culture Collection. A hybridoma-secreting antibody against the rat CD8 α chain (OX8) was obtained from the European Collection of Cell Cultures (Wiltshire, United Kingdom). mAbs against CD63 (LP9), CD81 (JS64), CD9 (MM2/57), and integrin α2 (AK7) were purchased from Serotec Ltd. (Oxford, United Kingdom). A hybridoma-producing antibody against a surface antigen on CL1-5 cells (Ly-5D7) was produced as described previously (27). FITC-conjugated goat antimouse immunoglobulin was from Organon Teknika (Durham, NC). Antibodies were purified from ascites fluid by protein-A affinity chromatography. L6 Fab fragments were produced by digesting mAb L6 (3 mg/ml) in 0.1 M Tris-HCl (pH 8.0), 2 mM EDTA, and 0.1 mM DTT with 0.03 mg/ml activated papain (Sigma Chemical Co., St. Louis, MO) for 3 h at 37°C. The reaction was terminated by addition of iodoacetamide to 2 mM. The flow-through from a protein-A affinity column was additionally purified on a Hiload 16/60 Superdex 75 pg column (Amersham Pharmacia Biotech Asia Pacific Ltd., Taiwan Branch Office, Taipei, Taiwan) equilibrated with PBS. L6 Fab antigen-binding activity was measured by competitive ELISA. Graded amounts of OX8, mAb L6, or L6 Fab were incubated with biotinylated mAb L6 (2 µg/ml) for 3 h in microtiter wells coated with CL1-5 cells. The cells were washed, and antibody binding was measured at 405 nm after addition of horseradish peroxidase-conjugated streptavidin (1:

1000; Jackson ImmunoResearch Laboratories, West Grove, PA) followed by 2,2'-azino-bis[3-ethylbenziazoline-6-sulfonic acid] substrate (28).

TAL6 Cell Transfectants. Human TAL6 cDNA was amplified by RT-PCR with primers P1, 5'-CCT AGG GAT CCA CCA TGT GCT ATG GGA AGT GTG CA-3' and P2, 5'-GGG TTG TCT AGA TTA GCA GTC ATA TTG CTG TTG GTG-3' from RNA isolated from CL1-5 cells as described (29). The PCR product was digested with *Bam*HI and *Xba*I restriction enzymes (italicized) and subcloned into pcdcf3 (generously provided by Dr. Jerome Langer, Robert Wood Johnson Medical School, Piscataway, NJ) under the control of the human polypeptide chain elongation factor 1α promoter (30). CL1-0 cells transfected with pcdcf3 or pcdcf3-L6 were selected in G418 (Calbiochem, San Diego, CA) to generate CL1-0/pdef and CL1-0/L6 cells, respectively. CL1-0/L6 cells were sorted for high expression of TAL6 on a fluorescence-activated cell sorter to produce CL1-0/L6-H cells.

Flow Cytometric Assay. Immunofluorescence staining of cells was performed as described (31). MF, measured on a FACScaliber flow cytometer (Becton Dickinson, Mountain View, CA), was calculated with FlowJo 3.2 (Tree Star, Inc., San Carlos, CA). RF was calculated as:

$$\text{RF (\%)} = 100 * \frac{\text{MF}_{\text{S/L6}} - \text{MF}_{\text{S/C}}}{\text{MF}_{\text{CL1-5/L6}} - \text{MF}_{\text{CL1-5/C}}}$$

where MF_{S/L6} and MF_{S/C} represent the MF of sample cells stained with mAb L6 or control antibody, respectively, and MF_{CL1-5/L6} or MF_{CL1-5/C} represent the MF of CL1-5 cells stained with mAb L6 and control mAb, respectively.

In Vitro Migration and Invasion Assays. Tumor cell migration and invasion were examined in a membrane invasion culture system. A polycarbonate membrane with 10-µm pores (Nucleopore Corp., Pleasanton, CA) was coated with 5 mg/ml BD Matrigel Basement Membrane Matrix (BD Biosciences, Bedford, MA) in PBS for invasion assays or with 100 µg/ml gelatin (Sigma Chemical Co.) for migration assays. The cells that invaded through the coated membrane in 48 h (invasion) or 6 h (migration) were counted as described previously (23). In some experiments, the indicated concentrations of mAb L6 or control antibodies were added with the cells and after 24 h (invasion assay). In clustering experiments, CL1-5 cells were incubated with 0.5 µg/ml mAb OX8 or L6 for 1 h before 5 µg/ml second antibody (GAM or GAR) was added. The treatment was repeated after 24 h. Each experiment, performed in triplicate or quadruplicate, was repeated at least three times.

Adhesion Assay. EIA high protein binding flat-bottomed 96-well plates (Corning Inc., Corning, NY) were coated overnight at 4°C with 50 µl/well human fibronectin (60 µg/ml), human vitronectin (2 µg/ml), mouse laminin (16 µg/ml), bovine collagen type I (80 µg/ml), or human collagen type IV (80 µg/ml). All of the proteins were purchased from Sigma Chemical Co. Control plates were uncoated (0% binding) or coated with poly L-lysine (100% binding). The plates were washed and blocked (except for poly L-lysine-coated wells) with 5% BSA. CL1-0 (4 × 10⁵/ml) or CL1-5 (6 × 10⁵/ml) cells in RPMI 1640 containing 0.5% NuSerum were added to wells with 10 µg/ml

L6 or control antibody. The plates were briefly shaken, centrifuged at $500 \times g$, and then incubated at 37°C for 30 min. Adherent cells were fixed with 10% formalin and stained with 1% Toluidine blue in 10% formalin overnight. The cells were extensively washed, air dried, and then lysed with 2% SDS. The absorbance of the wells was measured at 600 nm in a microplate reader. Cell binding was calculated as:

$$\text{Binding \%} = 100 \times \frac{A_S - A_B}{A_{\text{PLL}} - A_B}$$

where A_S is the absorbance of sample wells, A_B is the absorbance of BSA-blocked wells, and A_{PLL} is the absorbance of poly L-lysine-coated wells. Each experiment, performed with 8–16 replicates, was repeated at least three times.

Collagen Zymography. CL1-0/pdef, CL1-0/L6, and CL1-5 cells were grown to confluence in six-well plates. The monolayers were washed three times with PBS and cultured overnight in 1 ml of serum-free RPMI 1640 supplemented with $5 \mu\text{g/ml}$ L6 or HB65. The culture supernatant was centrifuged at $1000 \times g$ for 10 min to remove debris, and then $20 \mu\text{l}$ of the medium was mixed with $10 \mu\text{l}$ SDS PAGE sample buffer without reducing agent. The samples were electrophoresed in a 10.5% SDS-PAGE containing 1 mg/ml gelatin. The gel was washed in 50 mM Tris-HCl (pH 7.4) containing 2.5% Triton X-100 for 30 min. The gel was then incubated in activation buffer [50 mM Tris-HCl (pH 7.5), 150 mM NaCl, 10 mM CaCl_2 , and 0.05% NaN_3] for 24 h at 37°C . The gel was subsequently stained with Coomassie blue, and destained in water containing 10% methanol and 10% acetic acid.

Patients and Specimens. Fifty four patients who underwent surgery for non-small cell lung cancer at the National Taiwan University Hospital from September 1, 1994, through August 31, 1996, were included in the study. This investigation was performed after approval by the Institutional Review Board of the National Taiwan University Hospital. Written informed consent was obtained from all of the patients. None of the patients had received neoadjuvant chemotherapy or radiation therapy before surgery. Specimens of lung cancer tissue and adjacent normal lung tissue obtained at surgery were immediately snap-frozen in liquid nitrogen and stored at -80°C until use. WHO criteria (32) were used for histological classification. Tumor size, local invasion, and lymph node metastasis were determined at pathologic examination. The final disease stage was determined by a combination of surgical and pathologic findings, according to the current tumor-node-metastasis system for lung cancer staging (33). Among the 54 patients, 35 were men and 19 were women (mean age \pm SD = 62.4 ± 10.6 years), 22 of whom had squamous cell carcinoma and 32 of whom had adenocarcinoma. The surgical-pathology stage of disease was stage I in 19 patients, stage II in 9, stage III in 20, and stage IV in 6. Tumor status was T_1 in 11 patients, T_2 in 28, T_3 in 5, and T_4 in 10. Twenty-five patients had no lymph node metastasis (N_0), and 29 had regional or mediastinal lymph node metastasis (N_1 in 8 patients and N_2 in 21 patients). Follow-up data were obtained from the patient medical charts and from our tumor registry service. Follow-up times ranged from 32 to 81.8 months. Relapse time was calculated from the date of surgery to

the date of detection of local recurrence or systemic metastasis. Survival time was calculated from the date of surgery to the date of death. Patients who died of postoperative complications after surgery were excluded from the survival analysis.

Real-Time PCR. Total RNA was extracted from resected cancer tissue with an RNA extraction kit (RNeasy Mini Kit; Qiagen, Valencia, CA). The quality of RNA in samples was determined by electrophoresis through agarose gels and staining with ethidium bromide; 18S and 28S RNA bands were visualized with UV illumination. The samples used for the standard curve in the real-time quantitative RT-PCR were prepared by serial dilution to contain 250, 50, 10, and 2 ng of specific RNA. The serially diluted samples were distributed into aliquots and stored at -80°C until use. The primers used for L6 were as follows (34): forward primer = $5'\text{-cgtgtggtctttcttgcga-3}'$; reverse primer = $5'\text{-ccagcccaatgaagacaaatg-3}'$. The sequence of the probe used to detect and quantify the RT-PCR product was $5'\text{-tgccctgctgatgctct-3}'$. The probe was labeled at the 5' end with carboxyfluorescein and at the 3' end with N,N,N',N' -tetramethyl-6-carboxyrhodamine. The primers and probe used for quantitative RT-PCR of the TBP mRNA (internal control, GenBank accession no. X54993) were as described by Bieche *et al.* (35). The identities of PCR products were confirmed by DNA sequencing. Each amplification mixture ($50 \mu\text{l}$) contained 50 ng of sample RNA; $5 \times$ TaqMan EZ buffer ($10 \mu\text{l}$; Perkin-Elmer, Foster City, CA); 25 mM manganese acetate ($6 \mu\text{l}$); $300 \mu\text{M}$ AMP, deoxycytosine triphosphate, and dGTP; $600 \mu\text{M}$ dUTP; 5 units of *rTth* DNA polymerase; 0.5 units of AmpErase uracil *N*-glycosylase; 200 nM forward and reverse primer; and 100 nM dual-labeled fluorogenic probe (Perkin-Elmer). The *rTth* DNA polymerase has both reverse transcriptase and Taq polymerase activity. For reverse transcription, the mixtures were incubated at 50°C for 2 min, 60°C for 30 min, and 95°C for 5 min for deactivation. The subsequent thermal cycling profile consisted of 40 cycles of denaturation at 94°C for 20 s, and primer annealing and extension at 62°C for 1 min. Each assay included a standard curve, a no-template control, and triplicate total RNA samples. The fluorescence emitted by the reporter dye was detected on-line in real time with the ABI prism 7700 sequence detection system (PE Applied Biosystems). The C_T is the fractional cycle number at which the fluorescence generated by cleavage of the probe exceeds a fixed threshold above baseline. For a chosen threshold, a smaller starting copy number results in a higher C_T value. In this study, we used TBP mRNA as an internal control (35). The relative amount of tissue L6 mRNA, standardized against the amount of TBP mRNA, was expressed as $-\Delta C_T = -[C_{T(L6)} - C_{T(TBP)}]$. The ratio of the number of L6 mRNA copies to the number of TBP mRNA copies was then calculated as $2^{-\Delta C_T} \times K$, where K is a constant (36).

Experimental Metastasis. SCID mice obtained from the National Taiwan University were i.v. injected with 3×10^6 CL1-0, CL1-5, or CL1-0/L6-H cells in PBS. Mice survival was followed for 80 days. All of the animal experiments were carried out with prior approval by the Animal Committee of the Institute of Biomedical Sciences. The ethical guidelines that were followed met the standards required by the Interdisciplinary Principles and Guidelines for the Use of Animals in Research,

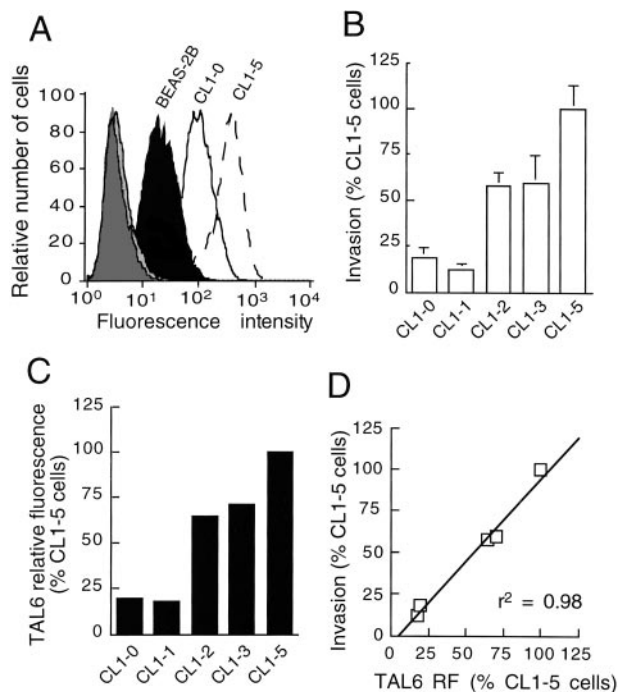


Fig. 1 TAL6 expression correlates with the *in vitro* invasiveness of CL lung cancer cells. **A**, immortalized normal human bronchial epithelial (filled curve), CL1-0 (—), and CL1-5 cells (---) were stained with mAb L6 or control mAb OX8 (shaded curves) and analyzed by flow cytometry. **B**, the invasion of CL lung carcinoma cells through membranes coated with Matrigel relative to the invasion of CL1-5 cells are shown. Bars, \pm SE. **C**, the RF of CL cell lines after staining with mAb L6 or control mAb was calculated as described in "Materials and Methods." **D**, linear regression analysis of the invasiveness of CL cell lines versus the RF of TAL6.

Testing, and Education issued by the New York Academy of Sciences' Ad Hoc Committee on Animal Research.

Statistical Analysis. Statistical significance of differences between mean values was estimated with Excel (Microsoft, Redmond, WA) using the independent *t* test for unequal variances. Statistical analysis of clinical data was performed using SPSS for Windows software (version 10.0; SPSS Inc., Chicago, IL). Fisher's exact tests and Student's *t* tests were used to compare the clinicopathologic characteristics of tumors (and patients) with high and low expression of L6 mRNA. Survival curves were obtained by the Kaplan-Meier method, and the difference in survival and relapse times between groups with low and high expression of L6 antigen was analyzed with the log-rank test. *Ps* < 0.05 were considered to be statistically significant.

RESULTS

Correlation between TAL6 Expression and Cell Invasiveness. Fig. 1A shows that mAb L6 against human TAL6 specifically stained immortalized normal human bronchial epithelial cells (MF = 25.3). TAL6 expression was elevated on CL1-0 lung carcinoma cells (MF = 110), whereas the more invasive CL1-5 lung carcinoma cells expressed even higher amounts of TAL6, suggesting a trend of increasing TAL6 ex-

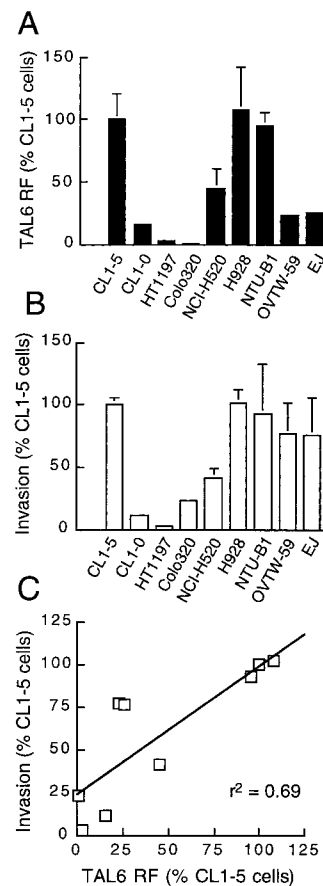


Fig. 2 Correlation of TAL6 expression with the *in vitro* invasiveness of human carcinoma cells. **A**, the RF of cells stained with mAb L6 or control mAb was calculated as described in "Materials and Methods." **B**, the invasion of cell lines through membranes coated with Matrigel relative to the invasion of CL1-5 cells is shown. Bars, \pm SE. **C**, linear regression analysis of the invasiveness of cell lines versus the RF of TAL6.

pression with malignancy. To additionally explore the relation between invasion and expression of TAL6, we quantified the invasiveness of five human lung carcinoma cell lines, CL1-0, CL1-1, CL1-2, CL1-3, and CL1-5 (Fig. 1B). The numbers of cells invading through a membrane coated with Matrigel were: CL1-0, 431 ± 144 ; CL1-1, 287 ± 79 ; CL1-2, 1350 ± 175 ; CL1-3, 1390 ± 360 ; and CL1-5, 2350 ± 300 , showing a general trend of increasing invasiveness. The RF of cell lines after staining with mAb L6 also displayed a trend of increasing TAL6 expression (Fig. 1C). Linear regression analysis revealed a strong correlation (correlation coefficient $r^2 = 0.98$) between invasion and expression of TAL6 on CL lung carcinoma cells (Fig. 1D).

The correlation between TAL6 expression and invasiveness was additionally explored in a panel of human carcinoma cell lines that included lung (CL1-0, CL1-5 NCI-H520, and H928), bladder (HT1197, NTU-B1, and EJ), colon (Colo320), and ovarian (OVTW-59) carcinoma cells. Fig. 2A shows that TAL6 RF values ranged from 0.6% on Colo320 cells to 108% on H928 cells. HT119 (98 \pm 35 cells) and CL1-0 (460 \pm 57

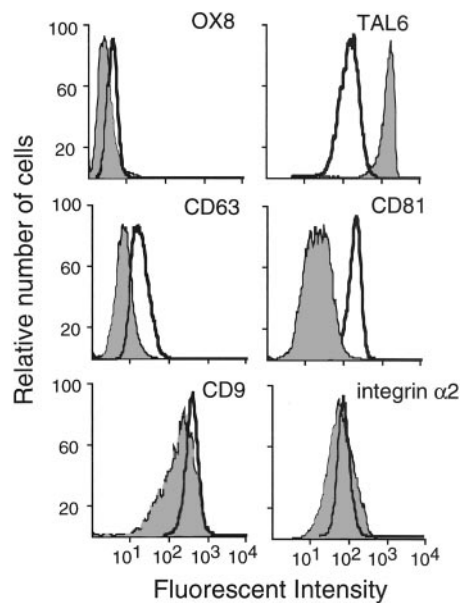


Fig. 3 Expression of tetraspanins on CL1-0 and CL1-5 cells. CL1-0 (open curves) and CL1-5 (shaded curves) cells were stained with control antibody (OX8) or mAbs against TAL6, integrin $\alpha 2$, or tetraspanins (CD9, CD63, and CD81).

cells) cell lines displayed the lowest invasion, whereas CL1-5 (4000 ± 232), H928 (4040 ± 420), and NTU-B1 (3700 ± 1600) cells were most invasive (Fig. 2B). Linear regression analysis revealed a trend ($r^2 = 0.69$) of increasing invasion as the level of TAL6 on the cells increased (Fig. 2C).

In contrast to the trend observed for TAL6 expression, many TM4SF members display a trend of decreased expression with increasing malignancy. To determine whether CL lung carcinoma cells atypically express TM4SF proteins, we performed immunofluorescence analysis of CL1-0 and CL1-5 cells with mAbs against the TM4SF members CD9, CD63, and CD81. Fig. 3 shows that slightly more CD9 was expressed on CL1-0 cells as compared with CL-5 cells. Similarly, both CD63 and CD81 were more highly expressed on CL1-0 cells than on CL1-5 cells. As before, TAL6 was more highly expressed on CL1-5 cells than on CL1-0 cells. The expression of a control protein (integrin $\alpha 2$) was similar on both CL1-0 and CL1-5 cells. These results demonstrate that CL lung carcinoma cells display the typical pattern of tetraspanin expression that is inversely correlated with malignancy.

Forced Expression of TAL6 Increases the Invasiveness of Lung Carcinoma Cells. A direct role for TAL6 in cancer cell invasion was investigated by engineering CL1-0 cells to express high levels of TAL6. CL1-0 cells were generated that expressed vector (CL1-0/pdef) or TAL6 (CL1-0/L6 cells). Transfected cells were also sorted for enhanced TAL6 expression (CL1-5/L6-H cells). Populations of cells were used in all of the experiments to eliminate possible artifacts associated with cell clones. Fig. 4A shows that TAL6 expression was highest on CL1-5 cells followed by CL1-0/L6-H and then CL1-0/pdef cells. CL1-0/L6 cells displayed TAL6 densities intermediate to CL1-0/pdef and CL1-0/L6-H (results not shown). The

doubling times of CL1-0/pdef, CL1-0/L6-H, and CL1-5 cells were similar (17.5, 17.9, and 18.0 h, respectively), demonstrating that forced expression of TAL6 did not affect cell viability or growth rate (Fig. 4B). Comparison of the adherence of CL1-0/pdef, CL1-0/L6-H, and CL1-5 cells to purified ECM proteins revealed that overexpression of TAL6 significantly ($P \leq 0.05$) increased CL1-0/L6-H cell adhesion to collagen type IV (Fig. 4C). However, this minor effect is of questionable biological significance. CL1-5 and CL1-0 cells displayed similar binding to fibronectin, laminin, and vitronectin, but significantly more CL1-5 cells adhered to collagen type I and collagen type IV. Interestingly, CL1-5 cells displayed significantly lower adhesion than CL1-0 cells to Matrigel, although collagen type IV is a major component of Matrigel. Fig. 4D illustrates that the invasiveness of CL1-0/L6 ($225\% \pm 18\%$) and CL1-0/L6-H ($257\% \pm 31\%$) cells was significantly ($P \leq 0.0005$) higher than CL1-0/pdef cells ($100\% \pm 4.1\%$). Investigation of ECM degradation showed that culture supernatant from CL1-5 cells possessed high collagenase activity as compared with CL1-0 cells (Fig. 4E). However, expression of TAL6 did not appear to be related to collagenase activity; neither addition of L6 antibody to cells nor expression of TAL6 on CL1-0 cells produced visible changes in collagenase activity. The *in vivo* malignancy of CL1-0/L6-H cells was also examined in an experimental metastasis model. Previous studies have demonstrated that *i.v.* injection of CL1-5 cells in SCID mice results in progressive growth of lung-tumor colonies with typical adenocarcinoma tumor morphology (25). Fig. 4F shows that mice *i.v.* injected with CL-0/L6-H cells exhibited a significant ($P \leq 0.05$) reduction in mean survival time (43.3 ± 3.0 days) compared with mice that were injected with CL1-0/pdef cells (57.8 ± 4.7 days). The mean survival time of mice injected with CL1-5 cells was additionally reduced (36.6 ± 4.0 days). There was no significant difference in the mean survival times of mice injected with CL-0/L6-H or CL1-5 cells. Taken together, these results suggest that high expression of TAL6 can increase both *in vitro* and *in vivo* cell invasiveness.

Anti-TAL6 Antibody Decreases Cancer Cell Invasion. Addition of mAb L6 to CL1-5 cells in the upper chamber of a membrane invasion chamber significantly ($P \leq 0.0005$) reduced their invasion by 41% as compared with cells treated with control mAb. mAb L6 also significantly ($P < 0.05$) reduced the migration of CL1-5 cells through a gelatin-coated membrane by $\sim 15\%$ as compared with control antibody (Fig. 5B). Suppression of cell invasion and migration by mAb L6 was not caused by inhibition of cell growth, because the doubling time of CL1-5 cells treated with L6 (20.9 h) was similar to cells treated with OX8, a nonbinding control antibody (22.8 h), or mAb Ly-5D7, an antibody that binds to an unidentified surface antigen on CL1-5 cells (23.8 h; Fig. 5C). In agreement with high TAL6 cell experiments, mAb L6 did not significantly alter the adhesion of CL1-5 cells to fibronectin, laminin, collagen type I, collagen type IV, or vitronectin (Fig. 5D).

To additionally investigate the mechanism of antibody modulation of cell invasion, the effect of antibody dose on the invasion of CL1-5 cells was examined. Fig. 6A shows that the invasion of CL1-5 cells was inhibited by mAb L6 in a dose-dependent fashion. CL1-5 invasion was inhibited significantly by concentrations of mAb L6 $> 2.5 \mu\text{g/ml}$. However, an inter-

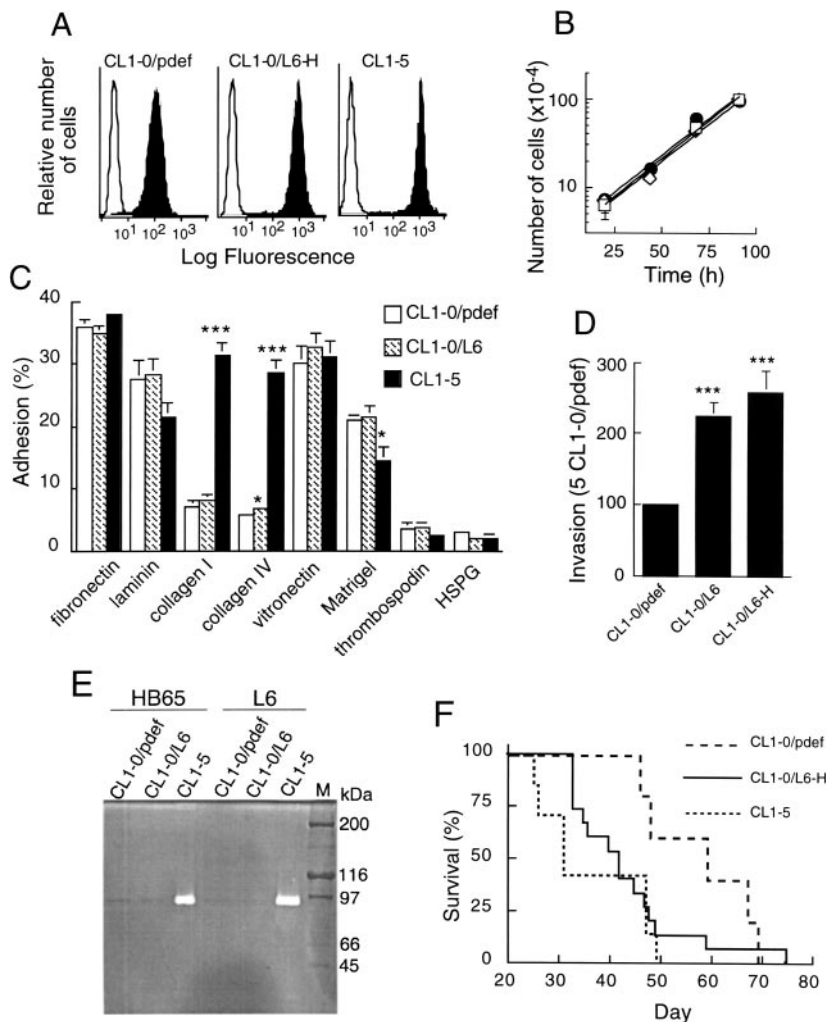


Fig. 4 Increased expression of TAL6 increases the invasiveness of lung carcinoma cells. **A**, CL1-5 cells and CL1-0 cells that expressed vector alone (*CL1-0/pdef*) or TAL6 (*CL1-0/L6-H*) were stained with control (open curves) or L6 antibody (filled curves). **B**, the numbers of CL1-0/pdef (□), CL1-0/L6-H (◇), and CL1-5 (●) cells were determined daily. **C**, adhesion of CL1-0/pdef (□), CL1-0/L6-H (▨), and CL1-5 (■) cells to ECM proteins. Results show the mean percentage of input cells that adhered. Significant differences between CL1-0/pdef and CL1-0/L6-H or CL1-5 cells are indicated; *, $P \leq 0.05$; ***, $P \leq 0.0005$. Bars, \pm SE. **D**, the invasion of CL1-0/L6 and CL1-0/L6-H cells through Matrigel relative to the invasion of CL1-0/pdef cells. Significant differences between CL1-0/pdef and the L6 transfectants are indicated; ***, $P \leq 0.0005$. Bars, \pm SE. **E**, collagen zymogram of supernatants collected from CL1-0/pdef, CL1-0/L6, or CL1-5 cells treated with mAb HB65 or L6 are shown. **F**, the survival of SCID mice after i.v. injection of CL1-0/pdef ($n = 5$), CL1-0/L6-H ($n = 15$), or CL1-5 ($n = 7$) cells. The mean survival time of CL1-0/L6-H mice was significantly ($P \leq 0.05$) shorter than CL1-0/pdef mice.

mediate concentration of mAb L6 (10 μ g/ml) inhibited the invasion of CL1-5 cell significantly ($P \leq 0.005$) more than did a high concentration (50 μ g/ml) of antibody. This result suggested that clustering of TAL6 on cells was required to inhibit cell invasion, because monovalent binding is favored at high antibody concentrations. To directly test whether TAL6 clustering was required to suppress invasion, we prepared monovalent Fab fragments of mAb L6. Purification of the Fab fragments to remove bivalent antibodies resulted in a single band on SDS PAGE under reducing conditions corresponding to the light chain, and variable and C_{H1} regions of the heavy chain (Fig. 6B). The L6 Fab fragments retained antigen-binding activity as demonstrated by their competition of biotinylated mAb L6 binding to CL1-5 cells (Fig. 6C). L6 Fab fragments did not significantly ($P > 0.35$) reduce the invasiveness of CL1-5 cells, confirming that TAL6 bridging was required to reduce cancer cell invasiveness (Fig. 6D). We also examined whether clustering of TAL6 could enhance suboptimal antibody stimulation of cells. Fig. 6E shows that CL1-5 cells incubated with a low concentration of L6 (0.5 μ g/ml) and a clustering second antibody (L6 + GAM) displayed significantly ($P \leq 0.05$) reduced

invasion compared with a nonclustering second antibody (L6 + GAR). The GAM second antibody did not directly inhibit CL1-5 invasion as shown by addition of control antibody with second antibody (OX8 + GAM). Taken together, these results demonstrate that clustering of TAL6 on the cell surface modulated cancer cell invasiveness.

Association of TAL6 mRNA Expression with Postoperative Relapse and Survival of Patients with Lung Cancer.

Real-time quantitative RT-PCR was used to measure the number of *TAL6* transcripts in lung cancer tissue from 54 patients with lung cancer. Tumor samples from lung cancer patients were arbitrarily classified as having either high or low *TAL6* expression with a cutoff value taken as the mean *TAL6* expression level from all of the patients. No relationship was seen between *TAL6* expression and clinicopathologic characteristics, including age, sex, stage of disease, lymph node status, and tumor histology (Table 1). The median survival of low-expression patients (50.1 months) was longer than the high-expression patients (33.2 months), but the difference was not significant by the log-rank test ($P = 0.234$; Fig. 7A). Comparison of the limited number of squamous cell carcinoma patients revealed

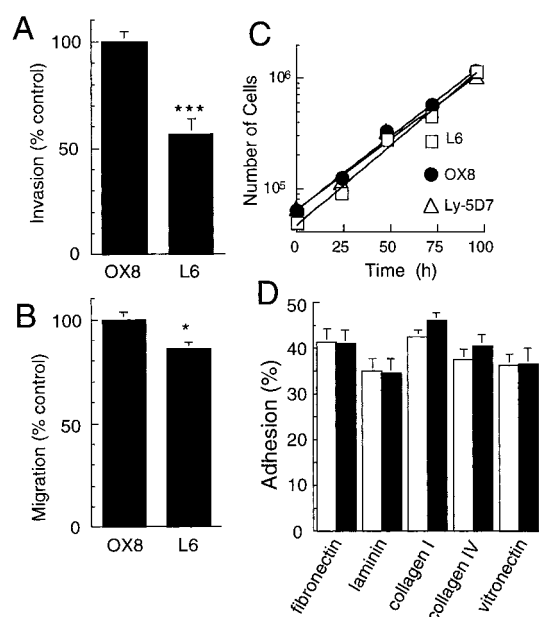


Fig. 5 mAb L6 affects the invasion and migration of lung carcinoma cells. **A**, invasion of CL1-5 cells through Matrigel in the presence of 20 $\mu\text{g/ml}$ control or L6 antibody. Bars, \pm SE. Significant differences between control and L6 antibodies are indicated: ***, $P \leq 0.0005$. **B**, migration of CL1-5 cells in the presence of 20 $\mu\text{g/ml}$ control or L6 mAb. Bars, \pm SE. Significant differences between control and L6 antibodies are indicated: *, $P \leq 0.05$. **C**, the number of CL1-5 cells cultured with mAb L6, OX8, or Ly-5D7 (20 $\mu\text{g/ml}$) was determined daily. **D**, the adhesion of CL1-5 cells to ECM proteins after addition of control (□) or L6 (■) mAbs. The percentage of input CL1-5 cells adhering to ECM proteins are indicated. Bars, \pm SE.

that the low-expression patients had statistically significant longer survival (median survival >61.7 months) as compared with the high-expression patients (median survival = 26.5 months; log-rank test, $P = 0.025$; Fig. 7B). The median duration to postoperative recurrence in squamous cell carcinoma patients was also significantly longer in low-expression patients (>61.7 months) as compared with the high-expression patients (16.2 months; log-rank test; $P = 0.034$).

DISCUSSION

TAL6 is widely distributed on the majority of human lung, colon, breast, and ovarian tumors (10), as well as on renal cell carcinomas (37) and prostate carcinoma cells (38). Although TAL6 has generated substantial interest as a target for cancer immunotherapy (19), antibody-directed enzyme prodrug activation (20), and radioimmunotherapy (21), little is known about the biological function of TAL6. Here we present several lines of evidence that implicate TAL6 in cancer metastasis. We found that expression of TAL6 on CL lung carcinoma cells correlated with the invasive capabilities of these cells. The expression of TAL6 also correlated with the invasiveness of several epithelial-derived tumors. A direct role for TAL6 in cancer metastasis was demonstrated in CL1-0 cells that were engineered to express high levels of TAL6. These cells displayed significantly increased invasiveness through Matrigel-coated membranes and enhanced malignancy in an experimental metastasis model in

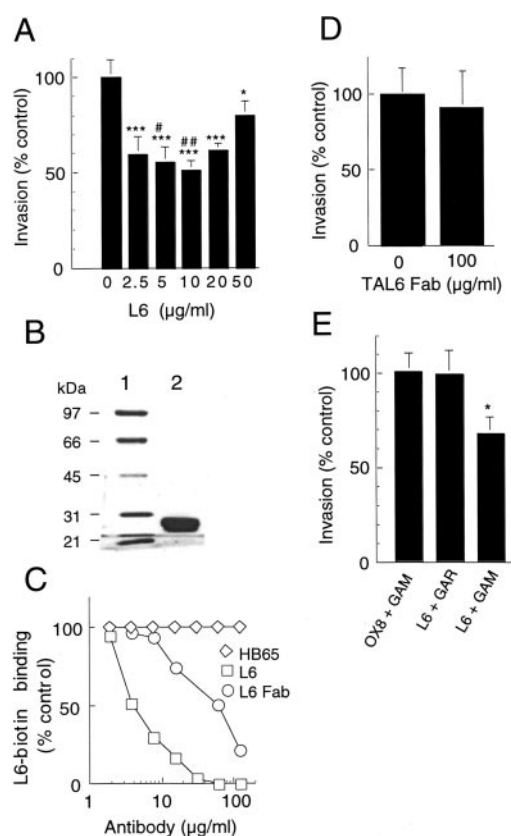


Fig. 6 Clustering of TAL6 is required to inhibit lung cancer invasion. **A**, invasion of CL1-5 cells through Matrigel in the presence of 0, 2.5, 5, 10, 20, or 50 $\mu\text{g/ml}$ mAb L6. Bars, \pm SE. Significant differences between invasion with and without mAb L6 are indicated: *, $P \leq 0.05$; ***, $P \leq 0.0005$. Significant differences between 50 $\mu\text{g/ml}$ mAb L6 and other antibody concentrations are indicated: #, $P \leq 0.05$; ##, $P \leq 0.005$. **B**, molecular weight markers (Lane 1) or L6 Fab fragments (Lane 2) were electrophoresed on a reducing SDS-PAGE. **C**, the competition of biotin-labeled mAb L6 for binding to CL-5 cells by the indicated concentrations of control mAb HB65 (100% binding), mAb L6, or L6 Fab are shown. **D**, invasion of CL1-5 cells through Matrigel with 0 or 100 $\mu\text{g/ml}$ L6 Fab. **E**, the invasion of CL1-5 cells through Matrigel after the addition of mAb OX8 or L6 (0.5 $\mu\text{g/ml}$) followed by clustering (GAM) or nonclustering (GAR) second antibodies. Bars, \pm SE. Significant differences between invasion with (L6 + GAM) and without (L6 + GAR) TAL6 clustering are indicated: *, $P \leq 0.05$.

mice. Conversely, clustering TAL6 molecules on CL1-5 cells with mAb L6 modulated cell migration and invasion. Finally, increased expression of TAL6 was associated significantly with early postoperative relapse and shorter survival in lung squamous cell carcinoma patients. Taken together, our results support the notion that TAL6 plays an important role in cancer invasion and metastasis.

We used a panel of lung carcinoma cells to explore possible relationships between TAL6 expression and cancer cell metastasis. This cell model was developed from a poorly differentiated lung carcinoma cell line (CL1-0) by selecting subpopulations of cells that displayed enhanced invasiveness in a transwell invasion chamber (25). The five sublines (CL1-0 to CL1-5) not only displayed progressively increasing invasive-

Table 1 Clinicopathologic characteristics of tumors with low and high expression of tumor-associated L6 antigen mRNA

Characteristic	-ΔCT		P
	<6.35	>6.35	
Age, y, mean ± SD	61 ± 11	64 ± 10	0.286 ^a
Sex, no. of patients			
Male	15	20	0.642
Female	10	9	
Stage, ^b no. of patients			
I-II	15	13	0.290
III-IV	10	16	
Tumor status, ^b no. of patients			
T ₁₋₂	19	20	0.762
T ₃₋₄	6	9	
Lymph node status, ^b no. of patients			
N ₀	12	13	1.00
N ₁₋₃	13	16	
Histology, no. of patients			
Squamous cell carcinoma	9	13	0.585
Adenocarcinoma	16	16	

^a Derived with Student's *t* test; other *P*s were derived with Fisher's exact test. All statistical tests were two sided.

^b Tumor stage, tumor status, and lymph node status were classified according to the International System for Staging Lung Cancer (33).

ness *in vitro*, but also exhibited a similar trend of greater metastatic potential in SCID mice (25) and enhanced invasiveness in a tracheal graft assay (23). We also showed that CL1-5 cells were more malignant than CL1-0 cells in a SCID mouse experimental metastasis model (Fig. 4F). Therefore, the CL1-0/CL1-5 cell model captures relevant biological characteristics for studying the metastatic behavior of lung cancer cells. TAL6 is a distant relative of the TM4SF that includes at least 25 members (39). This superfamily is distinguished by the presence of four hydrophobic transmembrane domains oriented such that the NH₂ and COOH termini are located intracellularly, and two loops are located extracellularly. TM4SF proteins exhibit promiscuous association with lineage-specific surface proteins, integrins, and other TM4SF members. In fact, many of the biological activities of TM4SF proteins are attributed to their association with integrins (40, 41). TM4SF proteins are thought to link integrins with cellular kinases and signaling molecules, thereby promoting lamellipodial extension and retraction (42). Tetraspanins have been nicknamed "molecular facilitators" to highlight their propensity to group specific cell-surface proteins, and enhance the formation and activity of signaling complexes (11).

TAL6 differs from most other TM4SF members in that it primarily influenced invasion, whereas most tetraspanins primarily act by modulating cell motility (39). The divergence of TAL6 function is also highlighted by the positive correlation of TAL6 expression with cancer cell invasion and poor patient prognosis. In contrast, the expression of most TM4SF members is inversely correlated with cancer cell metastasis and patient prognosis (16–18). Interestingly, PETA-3 (CD151) expression has also been positively correlated with cancer cell migration and metastasis (15). However, detailed analysis of conserved regions in TM4SF members indicates that TAL6 may belong to a new four-transmembrane superfamily comprising TAL6, IL-TMP, TM4SF5, and L6D (43).

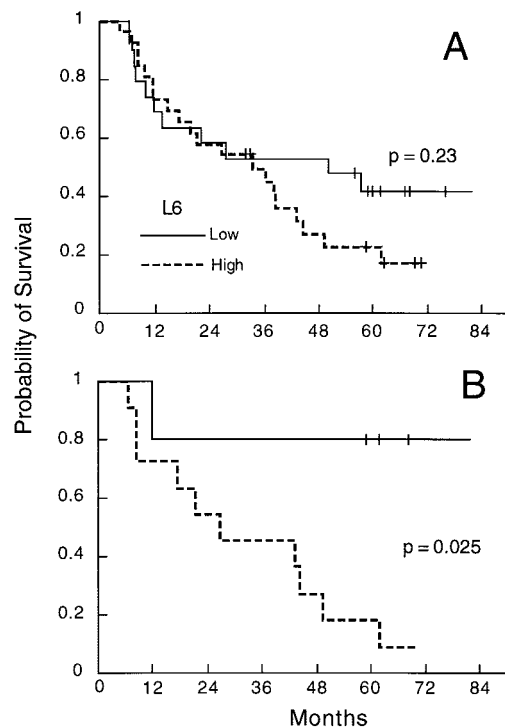


Fig. 7 Kaplan-Meier survival plots for patients with non-small cell lung cancer, grouped according to tumor-associated antigen TAL6 mRNA expression. The relative amount of tissue L6 mRNA, standardized against the amount of TATA-box-binding protein mRNA, was expressed as $-\Delta\text{CT} = -[\text{CT}(\text{L6}) - \text{CT}(\text{TBP})]$. Patients were included in the high-expression group when the $-\Delta\text{CT}$ value was ≥ 6.35 . A, difference in overall survival between high ($n = 26$) and low ($n = 19$) TAL6 expression groups among lung cancer patients was not significant ($P = 0.23$). B, the difference in overall survival between the high ($n = 11$) and low ($n = 5$) TAL6 expression groups among the limited number of patients with squamous cell carcinoma is statistically significant ($P = 0.025$). All of the patients alive at their last follow-up are indicated by tick marks on the plot.

Therefore, TAL6 may exert biological effects that are distinct from the "classical" tetraspanins.

One possible effector of TAL6 function is aminopeptidase N (CD13), which associates in a complex with TAL6 on the surface of human lung cancer cells.⁴ CD13 is a type II transmembrane Zn²⁺-dependent metalloproteinase that catalyzes the cleavage of neutral amino acids from the NH₂ terminus of peptides (44). CD13 expression has been correlated with the invasion of melanoma (45) and prostate carcinoma (46) cells. Although CD13 has been implicated in the activation of collagenase IV (47), we did not find any evidence that TAL6 modulated the collagenase activity of cancer cells (Fig. 4E). Antibody-mediated clustering of TAL6 modulated the invasiveness of CL1-5 cells, suggesting that TAL6 can initiate cell signaling. The PDZ protein SITAC/syntenin 2 α was shown recently to bind the peptide sequence Y-X-C-COOH at the COOH terminus of TAL6 (48). The syntenin-binding motif is conserved among

⁴ Manuscript in preparation.

human, hamster, and murine TAL6, suggesting a possible role for this interaction in TAL6 function.

Taken together, our results suggest that TAL6 plays a role in cancer cell invasion. Given the broad distribution of TAL6 on most epithelial-derived cancer cells, dissecting the molecular mechanisms of TAL6 modulation of cell invasion may provide new molecular targets for intervention or diagnosis of tumor cell metastasis.

ACKNOWLEDGMENTS

We thank Ya-Min Lin (Institute of Molecular Biology, Academia Sinica), and Wesley Roy Balasubramanian, Yu-Wen Chang, and Shuenn-Chen Yang (Institute of Biomedical Sciences, Academia Sinica) for technical assistance.

REFERENCES

- Woodhouse, E. C., Chuaqui, R. F., and Liotta, L. A. General mechanisms of metastasis. *Cancer (Phila.)*, *80*: 1529–1537, 1997.
- Christofori, G., and Semb, H. The role of the cell-adhesion molecule E-cadherin as a tumour-suppressor gene. *Trends Biochem. Sci.*, *24*: 73–76, 1999.
- Ziober, B. L., Lin, C. S., and Kramer, R. H. Laminin-binding integrins in tumor progression and metastasis. *Semin. Cancer Biol.*, *7*: 119–128, 1996.
- Akiyama, S. K., Olden, K., and Yamada, K. M. Fibronectin and integrins in invasion and metastasis. *Cancer Metastasis Rev.*, *14*: 173–189, 1995.
- Marshall, J. F., and Hart, I. R. The role of α v-integrins in tumor progression and metastasis. *Semin. Cancer Biol.*, *7*: 129–138, 1996.
- Kleiner, D. E., and Stetler-Stevenson, W. G. Matrix metalloproteinases and metastasis. *Cancer Chemother. Pharmacol.*, *43*: S42–S51, 1999.
- Zelinski, D. P., Zantek, N. D., Stewart, J. C., Irizarry, A. R., and Kinch, M. S. EphA2 overexpression causes tumorigenesis of mammary epithelial cells. *Cancer Res.*, *61*: 2301–2306, 2001.
- Muller, A., Homey, B., Soto, H., Ge, N., Catron, D., Buchanan, M. E., McClanahan, T., Murphy, E., Yuan, W., Wagner, S. N., Barrera, J. L., Mohar, A., Verastegui, E., and Zlotnik, A. Involvement of chemokine receptors in breast cancer metastasis. *Nature (Lond.)*, *410*: 50–56, 2001.
- Marken, J. S., Schieven, G. L., Hellstrom, I., Hellstrom, K. E., and Aruffo, A. Cloning and expression of the tumor-associated antigen L6. *Proc. Natl. Acad. Sci. USA*, *89*: 3503–3507, 1992.
- Hellstrom, I., Horn, D., Linsley, P., Brown, J. P., Brankovan, V., and Hellstrom, K. E. Monoclonal mouse antibodies raised against human lung carcinoma. *Cancer Res.*, *46*: 3917–3923, 1986.
- Maecker, H. T., Todd, S. C., and Levy, S. The tetraspanin superfamily: molecular facilitators. *FASEB J.*, *11*: 428–442, 1997.
- Ikeyama, S., Koyama, M., Yamaoko, M., Sasada, R., and Miyake, M. Suppression of cell motility and metastasis by transfection with human motility-related protein (MRP-1/CD9) DNA. *J. Exp. Med.*, *177*: 1231–1237, 1993.
- Radford, K. J., Thorne, R. F., and Hersey, P. Regulation of tumor cell motility and migration by CD63 in a human melanoma cell line. *J. Immunol.*, *158*: 3353–3358, 1997.
- Dong, J. T., Lamb, P. W., Rinker-Schaeffer, C. W., Vukanovic, J., Ichikawa, T., Isaacs, J. T., and Barrett, J. C. KAI1, a metastasis suppressor gene for prostate cancer on human chromosome 11p11.2. *Science (Wash. DC)*, *268*: 884–886, 1995.
- Testa, J. E., Brooks, P. C., Lin, J. M., and Quigley, J. P. Eukaryotic expression cloning with an antimetastatic monoclonal antibody identifies a tetraspanin (PETA-3/CD151) as an effector of human tumor cell migration and metastasis. *Cancer Res.*, *59*: 3812–3820, 1999.
- Higashiyama, M., Taki, T., Ieki, Y., Adachi, M., Huang, C. L., Koh, T., Kodama, K., Doi, O., and Miyake, M. Reduced motility related protein-1 (MRP-1/CD9) gene expression as a factor of poor prognosis in non-small cell lung cancer. *Cancer Res.*, *55*: 6040–6044, 1995.
- Adachi, M., Taki, T., Ieki, Y., Huang, C. L., Higashiyama, M., and Miyake, M. Correlation of KAI1/CD82 gene expression with good prognosis in patients with non-small cell lung cancer. *Cancer Res.*, *56*: 1751–1755, 1996.
- Miyake, M., Nakano, K., Itoi, S. I., Koh, T., and Taki, T. Motility-related protein-1 (MRP-1/CD9) reduction as a factor of poor prognosis in breast cancer. *Cancer Res.*, *56*: 1244–1249, 1996.
- Goodman, G. E., Hellstrom, I., Brodzinsky, L., Nicaise, C., Kulanter, B., Hummel, D., and Hellstrom, K. E. Phase I trial of murine monoclonal antibody L6 in breast, colon, ovarian, and lung cancer. *J. Clin. Oncol.*, *8*: 1083–1092, 1990.
- Svensson, H. P., Vruthula, V. M., Emswiler, J. E., MacMaster, J. F., Cosand, W. L., Senter, P. D., and Wallace, P. M. *In vitro* and *in vivo* activities of a doxorubicin prodrug in combination with monoclonal antibody β -lactamase conjugates. *Cancer Res.*, *55*: 2357–2365, 1995.
- Denardo, S. J., Richman, C. M., Goldstein, D. S., Shen, S., Salako, Q., Kukis, D. L., Meares, C. F., Yuan, A., Welborn, J. L., and Denardo, G. L. Yttrium-90/indium-111-DOTA-peptide-chimeric L6: pharmacokinetics, dosimetry and initial results in patients with incurable breast cancer. *Anticancer Res.*, *17*: 1735–1744, 1997.
- Tascou, S., Nayernia, K., Uedelhoven, J., Bohm, D., Jalal, R., Ahmed, M., Engel, W., and Burfeind, P. Isolation and characterization of differentially expressed genes in invasive and non-invasive immortalized murine male germ cells *in vitro*. *Int. J. Oncol.*, *18*: 567–574, 2001.
- Chen, J. J., Peck, K., Hong, T. M., Yang, S. C., Sher, Y. P., Shih, J. Y., Wu, R., Cheng, J. L., Roffler, S. R., Wu, C. W., and Yang, P. C. Global analysis of gene expression in invasion by a lung cancer model. *Cancer Res.*, *61*: 5223–5230, 2001.
- Storim, J., Friedl, P., Schaefer, B. M., Bechtel, M., Wallich, R., Kramer, M. D., and Reinartz, J. Molecular and functional characterization of the four-transmembrane molecule l6 in epidermal keratinocytes. *Exp. Cell Res.*, *267*: 233–242, 2001.
- Chu, Y. W., Yang, P. C., Yang, S. C., Shyu, Y. C., Hendrix, M. J., Wu, R., and Wu, C. W. Selection of invasive and metastatic subpopulations from a human lung adenocarcinoma cell line. *Am. J. Respir. Cell. Mol. Biol.*, *17*: 353–360, 1997.
- Reddel, R. R., Ke, Y., Gerwin, B. I., McMenamin, M. G., Lechner, J. F., Su, R. T., Brash, D. E., Park, J. B., Rhim, J. S., and Harris, C. C. Transformation of human bronchial epithelial cells by infection with SV40 or adenovirus-12 SV40 hybrid virus, or transfection via strontium phosphate coprecipitation with a plasmid containing SV40 early region genes. *Cancer Res.*, *48*: 1904–1909, 1988.
- Roffler, S. R., Chan, J., and Yeh, M. Y. Potentiation of radioimmunotherapy by inhibition of topoisomerase I. *Cancer Res.*, *54*: 1276–1285, 1994.
- Yeh, M. Y., Roffler, S. R., and Yu, M. H. Doxorubicin: monoclonal antibody conjugate for therapy of human cervical carcinoma. *Int. J. Cancer*, *51*: 274–282, 1992.
- Chou, W. C., Liao, K. W., Lo, Y. C., Jiang, S. Y., Yeh, M. Y., and Roffler, S. R. Expression of chimeric monomer and dimer proteins on the plasma membrane of mammalian cells. *Biotechnol. Bioeng.*, *65*: 160–169, 1999.
- Goldman, L. A., Cutrone, E. C., Kotenko, S. V., Krause, C. D., and Langer, J. A. Modifications of vectors pEF-BOS, pcDNA1 and pcDNA3 result in improved convenience and expression. *Biotechniques*, *21*: 1013–1015, 1996.
- Liao, K. W., Chou, W. C., Lo, Y. C., and Roffler, S. R. Design of transgenes for efficient expression of active chimeric proteins on mammalian cells. *Biotechnol. Bioeng.*, *73*: 313–323, 2001.
- The World Health Organization histological typing of lung tumours. Ed. 2. *Am. J. Clin. Pathol.*, *77*: 123–136, 1982.
- Mountain, C. F. Revisions in the International System for Staging Lung Cancer. *Chest*, *111*: 1710–1717, 1997.

34. Kaneko, R., Tsuji, N., Kamagata, C., Endoh, T., Nakamura, M., Kobayashi, D., Yagihashi, A., and Watanabe, N. Amount of expression of the tumor-associated antigen L6 gene and transmembrane 4 superfamily member 5 gene in gastric cancers and gastric mucosa. *Am. J. Gastroenterol.*, *96*: 3457–3458, 2001.
35. Bieche, I., Onody, P., Laurendeau, I., Olivi, M., Vidaud, D., Lide-reau, R., and Vidaud, M. Real-time reverse transcription-PCR assay for future management of ERBB2-based clinical applications. *Clin. Chem.*, *45*: 1148–1156, 1999.
36. Yuan, A., Yang, P. C., Yu, C. J., Chen, W. J., Lin, F. Y., Kuo, S. H., and Luh, K. T. Interleukin-8 messenger ribonucleic acid expression correlates with tumor progression, tumor angiogenesis, patient survival, and timing of relapse in non-small-cell lung cancer. *Am. J. Respir. Crit. Care Med.*, *162*: 1957–1963, 2000.
37. Svensson, H. P., Frank, I. S., Berry, K. K., and Senter, P. D. Therapeutic effects of monoclonal antibody- β -lactamase conjugates in combination with a nitrogen mustard anticancer prodrug in models of human renal cell carcinoma. *J. Med. Chem.*, *41*: 1507–1512, 1998.
38. O'Donnell, R. T., DeNardo, S. J., Shi, X. B., Mirick, G. R., DeNardo, G. L., Kroger, L. A., and Meyers, F. J. L6 monoclonal antibody binds prostate cancer. *Prostate*, *37*: 91–97, 1998.
39. Boucheix, C., and Rubinstein, E. Tetraspanins. *Cell Mol. Life Sci.*, *58*: 1189–205, 2001.
40. Indig, F. E., Diaz-Gonzalez, F., and Ginsberg, M. H. Analysis of the tetraspanin CD9-integrin α IIb β 3 (GPIIb-IIIa) complex in platelet membranes and transfected cells. *Biochem. J.*, *327*: 291–298, 1997.
41. Serru, V., Le Naour, F., Billard, M., Azorsa, D. O., Lanza, F., Boucheix, C., and Rubinstein, E. Selective tetraspan-integrin complexes (CD81/ α 4 β 1, CD151/ α 3 β 1, CD151/ α 6 β 1) under conditions disrupting tetraspan interactions. *Biochem. J.*, *340*: 103–111, 1999.
42. Woods, A., and Couchman, J. R. Integrin modulation by lateral association. *J. Biol. Chem.*, *275*: 24233–6, 2000.
43. Wright, M. D., Ni, J., and Rudy, G. B. The L6 membrane proteins—a new four-transmembrane superfamily. *Protein Sci.*, *9*: 1594–600, 2000.
44. Riemann, D., Kehlen, A., and Langner, J. CD13—not just a marker in leukemia typing. *Immunol. Today*, *20*: 83–88, 1999.
45. Menrad, A., Speicher, D., Wacker, J., and Herlyn, M. Biochemical and functional characterization of aminopeptidase N expressed by human melanoma cells. *Cancer Res.*, *53*: 1450–1455, 1993.
46. Ishii, K., Usui, S., Sugimura, Y., Yoshida, S., Hioki, T., Tatematsu, M., Yamamoto, H., and Hirano, K. Aminopeptidase N regulated by zinc in human prostate participates in tumor cell invasion. *Int. J. Cancer*, *92*: 49–54, 2001.
47. Fujii, H., Nakajima, M., Saiki, I., Yoneda, J., Azuma, I., and Tsuruo, T. Human melanoma invasion and metastasis enhancement by high expression of aminopeptidase N/CD13. *Clin. Exp. Metastasis*, *13*: 337–344, 1995.
48. Borrell-Pages, M., Fernandez-Larrea, J., Borroto, A., Rojo, F., Baselga, J., and Arribas, J. The carboxy-terminal cysteine of the tetraspanin L6 antigen is required for its interaction with SITAC, a novel PDZ protein. *Mol. Biol. Cell.*, *11*: 4217–4225, 2000.